

# Nonlinear absorption and refraction in CuCl at 532 nm

A. A. Said,\* T. Xia,<sup>†</sup> D. J. Hagan, and E. W. Van Stryland

*Center for Research and Education in Optics and Lasers, University of Central Florida, Orlando, Florida 32816*

M. Sheik-Bahae

*Department of Physics and Astronomy, University of New Mexico Albuquerque, New Mexico 87131*

Received April 1, 1996; revised manuscript received July 1, 1996

We report two-photon absorption in CuCl and its polarization dependence to give all three  $\chi^{(3)}$  tensor elements at 532 nm. We also report bound electronic  $n_2$  and free-carrier refraction in CuCl. The values obtained are each approximately one half the corresponding values for ZnSe. Previously, with ZnSe, the large two-photon absorption (2PA) and negative bound-electronic nonlinear refraction were combined with defocusing from 2PA-generated free carriers to provide effective optical limiting for visible picosecond input pulses. For nanosecond pulses thermal refraction is a problem because it leads to self focusing, and thus damage in ZnSe and most other semiconductors studied. However, the thermal refraction in CuCl is reported to be self-defocusing. Thus one might expect the self-protection properties of CuCl to be better than those of ZnSe for optical-limiting applications for nanosecond input pulses. © 1997 Optical Society of America [S0740-3224(97)02504-6]

## 1. INTRODUCTION

Copper chloride (CuCl) has a band-gap energy of  $E_g \approx 3.3\text{--}3.4$  eV (Ref. 1) at room temperature and therefore exhibits two-photon absorption (2PA) for wavelengths from  $\approx 740$  to  $\approx 350$  nm. For shorter wavelengths, bulk samples become opaque because of linear absorption. This wavelength range covers the entire visible spectrum, making this material ideally suited for visible sensor-protection (optical-limiting) applications. We report the 2PA coefficient  $\beta$ , the bound electronic nonlinear refractive index  $n_2$ , and the free-carrier nonlinear refractive cross section  $\sigma$ , in CuCl as obtained from Z-scan measurements with picosecond, 532-nm pulses. By measuring  $\beta$  for various linear polarization directions and with circular polarization, we determined all three  $\text{Im}\{\chi^{(3)}\}$  tensor elements (third-order electric susceptibility). Previous measurements of 2PA in CuCl are limited to uncalibrated nondegenerate spectra obtained with a combination of a fixed and a tuneable source,<sup>2–5</sup> luminescence spectra,<sup>5,6</sup> or 2PA spectra deduced from ellipse-rotation studies.<sup>7</sup> Of the experiments reporting calibrated values of  $\beta$ , values differ greatly;  $1 \times 10^6$  cm/GW,<sup>8</sup>  $3 \times 10^6$  cm/GW,<sup>9</sup> 45 cm/GW,<sup>10</sup> and 30 cm/GW.<sup>5</sup> Even the smallest of these values is significantly greater than that expected from scaling of data on a variety of other semiconductors.<sup>11,12</sup> Our polarization-dependent values are much smaller than previously reported ( $\approx 3$  cm/GW) and are consistent with well established theoretical predictions.<sup>11,12</sup>

Our interest in CuCl derives from our earlier work on nonlinearities in semiconductors.<sup>11–14</sup> There we verified predicted scaling relations for the 2PA coefficient with linear index, band-gap energy  $E_g$ , and photon energy  $\hbar\omega$ . From these scaling laws we obtained  $n_2$  by applying causality to obtain Kramers–Kronig relations between  $n_2$

and the ultrafast nonlinear absorption.<sup>15–17</sup> Examining these relations shows that for optical limiting applications in the visible, of the readily available wide-gap semiconductors, ZnS and ZnSe are excellent candidates.<sup>12–14</sup> Earlier work on these materials indeed showed that they worked well.<sup>13,14</sup> For example, a monolithic ZnSe limiter device showed a limiting threshold of  $\approx 10$  nJ for 30-ps, 532-nm pulses and was also demonstrated to be self-protecting; i.e., the bulk could not be damaged in a tight focusing geometry for more than a 4 orders-of-magnitude change in input.<sup>14</sup> The self-protecting property was due to the combination of nonlinear loss before the focus and the self-defocusing from the 2PA-induced free carriers.<sup>18–20</sup> Unfortunately, however, when subjected to nanosecond input pulses, optical damage was observed in the bulk of both ZnSe and ZnS. This damage was presumably due to the additional thermal nonlinearity occurring for longer input pulses. In most semiconductors the dominant thermal index change comes from the lowering of the band edge with temperature  $T$ , resulting in an increase of the index. This self-focusing opposes the carrier self-defocusing sufficiently to result in catastrophic damage. CuCl is one of the few semiconductors in which the band-gap energy is reported to increase with  $T$ .<sup>21,22</sup> In addition, examining the scaling relations for the nonlinearities of this material indicates that the nonlinear parameters are comparable with those of ZnS and slightly smaller than those of ZnSe, thus making it a good candidate for optical limiting in the visible for pulses from picoseconds to perhaps tens of nanoseconds.

## 2. NONLINEAR ABSORPTION

We used a mode-locked and Q-switched Nd:YAG laser with a single-pulse switch-out device that, when fre-

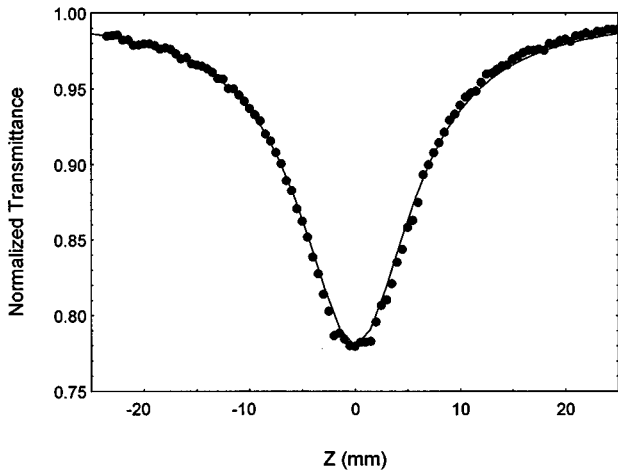


Fig. 1. Open aperture Z scan taken at an input irradiance of  $I_0 = 1.2 \text{ GW/cm}^2$ . The solid curve is a fit to the data.

quency doubled, gives 28-ps (FWHM) Gaussian temporal shaped pulses at 532 nm. The laser beam was measured to have a near-diffraction-limited Gaussian spatial profile, and the pulse width was monitored for each laser pulse.<sup>11,23,24</sup> The Gaussian beam was focused to a measured spot size  $w_0$  (half-width at the  $1/e^2$  maximum in irradiance) of  $30 \mu\text{m}$  for the Z-scan<sup>25,26</sup> experiments. To prevent the deterioration of the CuCl sample that occurs when it is exposed to the atmosphere (oxygen), the 2.4-mm-thick sample was immersed in a cuvette filled with carbon tetrachloride. Independent measurements of the liquid-filled cell without the CuCl showed that the nonlinear contributions from the carbon tetrachloride and the cell windows were negligible in these experiments.

We first performed open-aperture Z-scans to determine  $\beta$  by fitting the data to the following equation after performing spatial and temporal integrals over the radial distance  $r$  and time  $t$ ;

$$\frac{dI(z, z', r, t)}{dz'} = -\beta I^2(z, z', r, t) - \sigma_a N(z, z', r, t) I(z, z', r, t), \quad (1)$$

where  $z$  is the sample position with respect to the beam waist and  $z'$  is the depth within the sample. The second term gives the free-carrier absorption contribution to the absorption, where  $\sigma_a$  is the free-carrier absorption cross section and  $N$  the density of free carriers generated by 2PA. The carrier generation rate is given by

$$\frac{dN}{dt} = \frac{\beta I^2}{2\hbar\omega}, \quad (2)$$

where population relaxation mechanisms may be ignored on the 30-ps timescale of the laser pulse. The residual linear absorption coefficient is less than  $\approx 0.2 \text{ cm}^{-1}$ , so we may neglect any possible one-photon carrier generation processes. To make sure that the free-carrier absorption resulting from carriers produced by 2PA is negligible,<sup>1</sup> open-aperture Z-scans were performed at five input irradiances from 0.2 to  $1.5 \text{ GW/cm}^2$ . The same  $\beta$  value of  $\approx 2.9 \text{ cm/GW}$  was obtained to within  $\pm 10\%$  for all these measurements. This  $\pm 10\%$  uncertainty is a relative value, whereas we estimate our absolute uncertainty at

approximately  $\pm 20\%$ . One of these open-aperture Z-scans at an input irradiance of  $I_0 = 1.2 \text{ GW/cm}^2$  is shown in Fig. 1. Fitting of Eqs. (1) and (2) to the data gives an upper limit on  $\sigma_a$  of  $\approx 1 \times 10^{-17} \text{ cm}^2$ . In these measurements the sample is oriented such that the  $\mathbf{k}$  vector is parallel to the [001] crystallographic axis and  $\mathbf{E}$  is parallel to the [110] axis. Therefore we obtain  $\beta_{[110]} \approx 2.9 \pm 0.3 \text{ cm/GW}$ . The theoretical value of  $\beta$ , predicted from a simple two-parabolic-band model following the work of Wherrett,<sup>27</sup> is  $\beta = 4.6 \text{ cm/GW}$ .<sup>11</sup> This model does not include higher bands that contribute to the anisotropy of  $\beta$  as determined below.

### 3. ANISOTROPY OF $\beta$

The measurement of the anisotropy of 2PA in CuCl is performed by placing the sample at the minimum transmittance point in Z of the Z-scan, i.e., at focus, with the aperture open. A half-wave plate is placed before the focusing lens in the path of the beam. Rotation of the half-wave plate changes the incident angle of polarization. This measurement is explicitly detailed in Ref. 28. CuCl belongs to the symmetry group  $43m$ . The sample cut is such that the incident  $\mathbf{k}$  vector is parallel to the [001] crystallographic axis. Defining the input field as  $\mathbf{E} = E_0(\cos \theta)\mathbf{x} + E_0(\sin \theta)\mathbf{y}$ , where  $\theta$  is measured relative to the [100] axis, and the nonlinear polarization as  $\mathbf{P} = (1/2)\epsilon_0\chi_{\text{eff}}^{(3)}(\omega: -\omega, \omega, \omega)\mathbf{E}_0^3$ , we find the effective  $\chi^{(3)}$  is given by the following equation<sup>28-33</sup>:

$$\chi_{\text{eff}}^{(3)}(\theta) = \chi_{xxxx}^{(3)}[1 - (\sigma/2)\sin^2(2\theta)], \quad (3)$$

where  $\sigma$  is the coefficient of anisotropy given by

$$\sigma = 1 - \frac{[\chi_{xxyy}^{(3)} + 2\chi_{xyyx}^{(3)}]}{\chi_{xxxx}^{(3)}}. \quad (4)$$

Here we use the conventions of Ref. 16. In Fig. 2 we show the transmittance change  $\Delta T$  as a function of the polarization angle  $\theta$  at an input irradiance of  $\approx 1 \text{ GW/cm}^2$ . The solid curve in Fig. 2 is a least-squares fit to the data, which gives  $\sigma = -0.36 \pm 0.05$  and  $\beta_{[100]} = \beta_{[010]} \approx 2.5 \pm 0.3 \text{ cm/GW}$ . This corresponds to  $\text{Im} \chi_{xxxx}^{(3)} \approx (1.4$

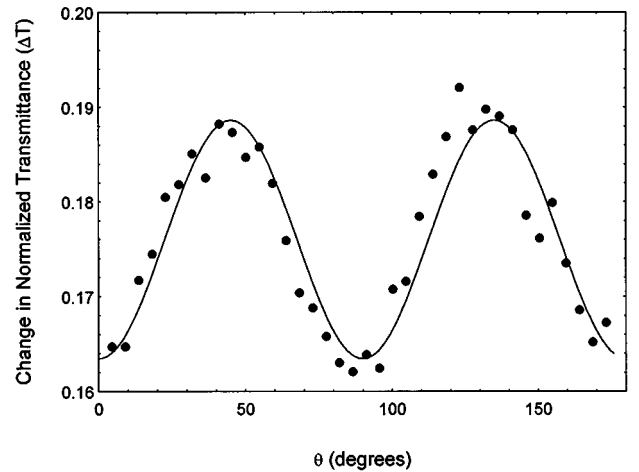


Fig. 2. Transmittance change  $\Delta T$  as a function of the polarization angle  $\theta$  measured relative to the [100] axis at an input irradiance of  $\approx 1 \text{ GW/cm}^2$ . The solid curve is a fit to the data.

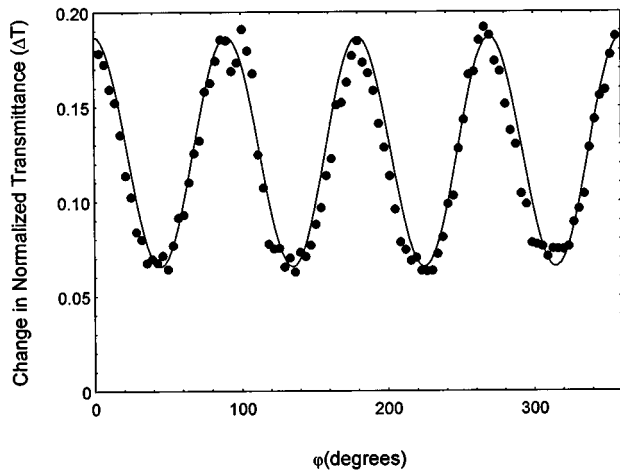


Fig. 3. Transmittance change  $\Delta T$  as a function of the angle of a  $\lambda/4$  wave plate at an input irradiance of  $1 \text{ GW/cm}^2$ . The solid curve is a fit to the data.

**Table 1. Two-Photon Absorption Coefficients,  $\beta$  (cm/GW), and  $\text{Im}\{\chi^{(3)}\}$  ( $\times 10^{-16} \text{ cm}^2/\text{V}^2$ ) Values**

$\beta_{[100]}$	$2.5 \pm 0.3$
$\beta_{[110]}$	$2.9 \pm 0.3$
$\beta_{\text{cir}}$	$0.87 \pm 0.09$
$\chi_{1111}^{(3)}$	$1.4 \pm 0.2$
$\chi_{1221}^{(3)}$	$0.37 \pm 0.06$
$\chi_{1122}^{(3)}$	$1.1 \pm 0.2$

$\pm 0.2) \times 10^{-16} \text{ cm}^2/\text{V}^2$ , where we have used the following relation between  $\beta$  and  $\chi^{(3)}$  in MKS:

$$\begin{aligned} \beta(m/W) &= \frac{3\omega}{2c^2 n_0^2 \epsilon_0} \text{Im}\{\chi^{(3)}(\omega; -\omega, \omega, \omega)\} \\ &= \mathbf{K} \text{Im}\{\chi^{(3)}(\omega; -\omega, \omega, \omega)\}, \end{aligned} \quad (5)$$

defining  $\mathbf{K}$  as used below. For circular polarization the analogous relations become

$$\chi_{\text{eff cir}}^{(3)} = \frac{1}{2} [\chi_{xxxx}^{(3)} + 2\chi_{xyyx}^{(3)} - \chi_{xxyy}^{(3)}]. \quad (6)$$

We determine  $\beta$  for circular polarization by measuring transmittance as the polarization is continuously varied between linear and circular polarization and back. This is accomplished by rotating a  $\lambda/4$ -wave plate with proper orientation to give the ratio of  $\beta_{\text{cir}}/\beta_{[110]}$  (i.e., field parallel to  $[110]$  in the absence of the  $\lambda/4$ -wave plate and  $\mathbf{k}$  parallel to  $[001]$ ). Figure 3 shows  $\Delta T$  as a function of the rotation angle  $\phi$  of the  $\lambda/4$ -wave plate, where  $\phi = 0$  corresponds to linear polarization in the  $[110]$  direction and  $\phi = 45^\circ$  corresponds to circular polarization. This gives  $\beta_{\text{cir}} = 0.87 \pm 0.09 \text{ cm/GW}$ . With the three values of  $\beta$ ,  $\beta_{\text{cir}}$ ,  $\beta_{[100]}$ , and  $\beta_{[110]}$ , listed in Table 1 we can unambiguously determine all three nonzero  $\chi^{(3)}$  tensor elements by using<sup>30</sup>

$$\sigma = 2(\beta_{[100]} - \beta_{[110]})/\beta_{[100]},$$

$$\text{Im}\{\chi_{xxxx}^{(3)}\} = 1/\mathbf{K} \beta_{[100]},$$

$$\text{Im}\{\chi_{xyyx}^{(3)}\} = 1/2\mathbf{K} (\beta_{[110]} - \beta_{[100]} + \beta_{\text{cir}}),$$

$$\text{Im}\{\chi_{xxyy}^{(3)}\} = 1/\mathbf{K} (\beta_{[110]} - \beta_{\text{cir}}). \quad (7)$$

The  $\chi^{(3)}$  values are listed in Table 1. This information can also be used to obtain information on higher energy bands.<sup>31,32</sup>

#### 4. NONLINEAR REFRACTION

Closed-aperture Z-scans were performed at several input irradiance levels to help determine the refractive nonlinearities. Nonlinear refraction in CuCl can arise from the electronic Kerr effect and also from band blocking<sup>34</sup> that is due to the generation of free carriers. The corresponding phase change with depth  $z'$  is described by

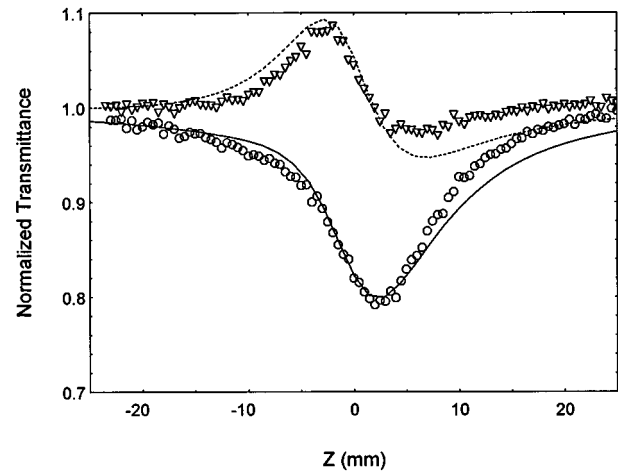


Fig. 4. Closed-aperture Z-scan data (circles) and closed-aperture data divided by open-aperture data (triangles) at an input irradiance of  $1.2 \text{ GW/cm}^2$ . The theoretical fit (solid and dashed curves) includes 2PA and  $n_2$  only.

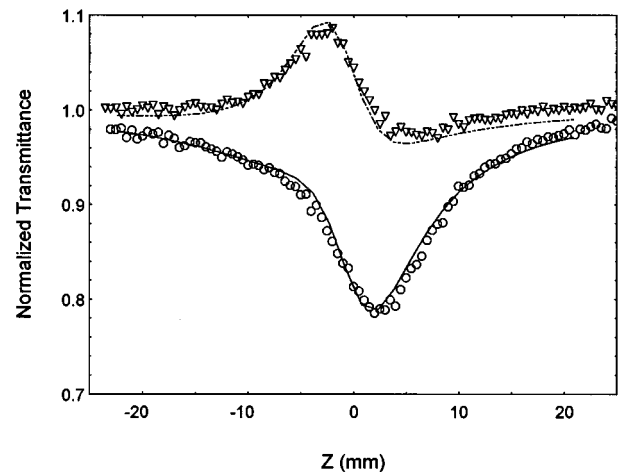


Fig. 5. Closed-aperture Z-scan data (circles) and closed-aperture data divided by open-aperture data (triangles) at an input irradiance of  $1.2 \text{ GW/cm}^2$ . The theoretical fit (solid and dashed curves) includes 2PA and both  $n_2$  and free-carrier refraction  $\sigma_r$ .

$$\frac{d\Phi}{dz'} = n_2 I + \sigma_r N, \quad (8)$$

where  $\sigma_r$  is the refractive-index change per carrier. As the carriers are generated by 2PA, the refraction caused by these carriers is a fifth-order nonlinearity compared with the third-order electronic Kerr contribution,  $n_2 I$ .<sup>22</sup> First an attempt was made to fit the experimental data by considering only the contribution of the third-order Kerr effect [first term in Eq. (8)]. Figure 4 shows the closed-aperture Z-scan data. Nonlinear absorption can be effectively removed by dividing the closed-aperture Z-scan data by open-aperture data.<sup>26</sup> This is also shown in Fig. 4. The lines are fits by use of Eq. (8) but neglecting the second term, i.e., with  $\sigma_r = 0$ . The best fit is obtained with an  $n_2$  value of  $-1.8 \times 10^{-14}$  cm<sup>2</sup>/W ( $-8.4 \times 10^{-12}$  esu). However, a much better fit of the same experimental data is obtained when both the Kerr nonlinearity and the free-carrier nonlinearities are considered. Using the five different closed-aperture Z-scans at various input irradiances from 0.2 to 1.5 GW/cm<sup>2</sup>, we find a best fit by using  $n_2 = -4.6 \times 10^{-16}$  cm<sup>2</sup>/W ( $-2.2 \times 10^{-13}$  esu) and  $\sigma_r = -4.5 \pm 0.5 \times 10^{-22}$  cm<sup>3</sup> in Eq. (8). A corresponding fit to one of the Z-scans is shown in Fig. 5. In fact, the carrier effect is the dominant term in Eq. (8), so that we can put bounds only on the magnitude of  $n_2$  of from nearly 0 to  $-0.13 \times 10^{-14}$  cm<sup>2</sup>/W ( $-0.6 \times 10^{-12}$  esu), although the sign is clearly negative. The value of  $n_2$  given by the theoretical model of the Kerr effect in semiconductors given by Sheik-Bahae *et al.*<sup>16,35</sup> using  $E_g = 3.35$  eV is  $n_2 = -0.17 \times 10^{-14}$  cm<sup>2</sup>/W ( $-0.8 \times 10^{-12}$  esu), but it is rapidly changing at this wavelength, as theory predicts a zero crossing of  $n_2$  at 532 nm for  $E_g = 3.39$  eV. The predictions are certainly consistent with the measured bound-electronic response.<sup>16</sup>

We compare the measured free-carrier effect to the simple two-band model by Aronov *et al.*<sup>36</sup> and Austin *et al.*<sup>37</sup> This model and other band-blocking models are explicitly discussed in Ref. 19. The calculated value obtained from the theory is  $\sigma_r = -2.7 \times 10^{-22}$  cm<sup>3</sup>, a factor of approximately two smaller than measured.

## 5. CONCLUSION

We have measured the third- and the fifth-order nonlinear optical effects in CuCl occurring for picosecond inputs at 532 nm. This information on the nonlinear optical parameters is important in assessing the feasibility of using CuCl in optical-limiting and optical-switching applications. The nonlinear coefficients are approximately one-half as large as the corresponding coefficients for ZnSe at the same wavelength.<sup>19</sup> ZnSe worked very well for picosecond pulses but suffered from thermally induced self-focusing damage for nanosecond pulses. For ZnSe and ZnS the band-gap shifts with temperature ( $dE_g/dT$ ) are  $-4.8 \times 10^{-4}$  and  $-4.7 \times 10^{-4}$  eV/K, respectively.<sup>38</sup> The value for CuCl is reported to be  $+1.3 \times 10^{-4}$  eV/K.<sup>21</sup> For most semiconductors the reduction of the band-gap energy with temperature raises the index of refraction, giving rise to thermal self focusing and optical damage. CuCl has the potential to protect optical elements from damage for pulses ranging from picoseconds to tens of

nanoseconds by using the combined electronic and thermal nonlinearities. Further work on the nonlinearities for longer input pulses is needed. In particular, the self-protecting properties of this material should be tested for nanosecond input pulses. This will require good optical-quality samples of several millimeter's thickness, which are not, to our knowledge, currently available. In addition, as discussed in Refs. 31 and 32, both the anisotropy in the values of  $\beta$  and the values of the tensor elements depend on higher bands; thus this information could in principle be used to refine our knowledge of the band structure of CuCl. However, the value of  $\sigma$  predicts a higher band at  $E'_g \approx 18$  eV (energy difference between higher band and valence band) from the relation  $\sigma \approx -2E_g/E'_g$ .<sup>30-32</sup> We do not have an explanation of why this value is so large. As discussed in detail in Ref. 11, there are numerous reasons for previous measurements<sup>5,8-10</sup> obtaining values for  $\beta$  larger than those reported here. These reasons range from using long pulses where free-carrier absorption dominates to not collecting all of the transmitted energy due to self lensing. Therefore the low values of  $\beta$  measured here, which are consistent with a simple theory shown to accurately predict 2PA coefficients in a variety of materials, should not be considered unusual.<sup>11,27</sup>

## ACKNOWLEDGMENTS

We gratefully acknowledge the support of National Science Foundation grants ECS-9510046 and 9320308 and the Naval Air Warfare Center Joint Service Agile Program contract N66269-C-93-0256. In addition we are grateful to J. B. Grün and the Service d'Elaboration et de Caractérisation des Matériaux for supplying the CuCl sample.

\*Present address: AccuPhotonics, Inc., 2901 Hubbard Road, Ann Arbor, Michigan 48105.

†Present address: Department of Electrical Engineering, University of Michigan, 1301 Beal Avenue, Ann Arbor, Michigan 48109.

## REFERENCES

1. K. H. Hellwege, ed., *Landolt-Börnstein Numerical Data and Functional Relationships in Science and Technology*, Vol. 17, Subvol. (b) of *Semiconductors* (Springer-Verlag, New York, 1982).
2. D. Fröhlich, B. Staginnus, and E. Schönherr, "Two-photon absorption spectrum of CuCl," *Phys. Rev. Lett.* **19**, 1032 (1967).
3. A. Bivas, C. Marange, J. B. Grün, and C. Schwab, "Two-photon absorption in CuCl," *Opt. Commun.* **6**, 142 (1972).
4. D. Fröhlich and H. Volkenandt, "Determination of  $\Gamma_3$  valence band in CuCl by two-photon absorption," *Solid State Commun.* **43**, 189 (1982).
5. I. M. Catalano, R. Cingolani, and M. Lepore, "Spectral behaviour of the two-photon absorption coefficient in ZnO, CuCl, and Bi<sub>4</sub>Ge<sub>3</sub>O<sub>12</sub>," *Nuovo Cimento* **9D**, 1313 (1987).
6. I. M. Catalano, A. Cingolani, R. Cingolani, and M. Lepore, "Interband two-photon absorption mechanisms in direct and indirect gap materials," *Phys. Scr.* **37**, 579 (1988).
7. M. Kuwata and N. Nagasawa, "Self-induced polarization rotation effect of an elliptically polarized beam in CuCl," *J. Phys. Soc. Jpn.* **51**, 2591 (1982).
8. G. M. Gale and A. Mysyrowicz, "Direct creation of excitonic

- molecules in CuCl by giant two-photon absorption," *Phys. Rev. Lett.* **32**, 727 (1974).
9. A. Bivas, R. Levy, V. D. Phach, and J. B. Grun, "Biexciton two-photon absorption in the nanosecond and picosecond range in copper halides," in *Physics of Semiconductors 1978*, Institute of Physics Conference Series No. 43 (American Institute of Physics, New York, 1979).
  10. G. Kobbe and C. Klingshrin, "Quantitative investigation of the two-photon absorption of ruby-laser-light in various semiconductors," *Z. Phys.* **B37**, 9 (1980).
  11. E. W. Van Stryland, H. Vanherzeele, M. A. Woodall, M. J. Soileau, A. L. Smirl, S. Guha, and T. F. Boggess, "Two photon absorption, nonlinear refraction, and optical limiting in semiconductors," *Opt. Eng.* **24**, 613 (1985).
  12. T. F. Boggess, A. L. Smirl, S. C. Moss, I. W. Boyd, and E. W. Van Stryland, "Optical limiting by two-photon absorption and nonlinear refraction in GaAs," *IEEE J. Quantum Electron.* **QE21**, 488 (1985).
  13. E. W. Van Stryland, Y. Y. Wu, D. J. Hagan, M. J. Soileau, and K. Mansour, "Optical limiting with semiconductors," *J. Opt. Soc. Am. B* **5**, 1980 (1988).
  14. D. J. Hagan, E. W. Van Stryland, M. J. Soileau, and Y. Y. Wu, "Self-protecting semiconductor optical limiters," *Opt. Lett.* **13**, 315 (1988).
  15. M. Sheik-Bahae, D. J. Hagan, and E. W. Van Stryland, "Dispersion and band-gap scaling of the electronic Kerr effect in solids associated with two-photon absorption," *Phys. Rev. Lett.* **65**, 96 (1989).
  16. M. Sheik-Bahae, D. Hutchings, D. J. Hagan, and E. W. Van Stryland, "Dispersion of bound electronic nonlinear refraction in solids," *IEEE J. Quantum Electron.* **27**, 1296 (1991).
  17. D. C. Hutchings, M. Sheik-Bahae, D. J. Hagan, and E. W. Van Stryland, "Kramers-Kronig relations in nonlinear optics," *Opt. Quantum Electron.* **24**, 1 (1992).
  18. E. J. Canto-Said, D. J. Hagan, J. Young, and E. W. Van Stryland, "Degenerate four-wave mixing measurements of high order nonlinearities in semiconductors," *IEEE J. Quantum Electron.* **QE-27**, 2274 (1991).
  19. A. A. Said, M. Sheik-Bahae, D. J. Hagan, T. H. Wei, J. Wang, J. Young, and E. W. Van Stryland, "Determination of bound and free-carrier nonlinearities in ZnSe, GaAs, CdTe, and ZnTe," *J. Opt. Soc. Am. B* **9**, 405 (1992).
  20. J. Wang, M. Sheik-Bahae, A. A. Said, D. J. Hagan, and E. W. Van Stryland, "Time-resolved Z-scan measurements of optical nonlinearities," *J. Opt. Soc. Am. B* **11**, 1009 (1994).
  21. Raga, *J. Phys. (Paris)* **28**, C3-116 (1967); Nasser Peyghambarian, Optical Sciences Center, University of Arizona, Tucson, Arizona 85721 (personal communication, 1994).
  22. N. Peyghambarian, S. Koch, and A. Mysyrowicz, *Introduction to Semiconductor Optics* (Prentice-Hall, New Jersey, 1993).
  23. W. H. Glen and M. J. Brienza, "Time evolution of picosecond optical pulses," *Appl. Phys. Lett.* **10**, 221 (1967).
  24. J. H. Bechtel and W. L. Smith, "Two-photon absorption in semiconductors with picosecond pulses," *Phys. Rev. B* **13**, 3515 (1976).
  25. M. Sheik-Bahae, A. A. Said, and E. W. Van Stryland, "Highsensitivity, single beam  $n_2$  measurement," *Opt. Lett.* **14**, 955 (1989).
  26. M. Sheik-Bahae, A. A. Said, T. H. Wei, D. J. Hagan, and E. W. Van Stryland, "Sensitive measurement of optical nonlinearities using a single beam," *IEEE J. Quantum Electron.* **26**, 760 (1990).
  27. B. S. Wherrett, "Scaling rules for multiphoton interband absorption in semiconductors," *J. Opt. Soc. Am. B* **1**, 67 (1984).
  28. R. DeSalvo, M. Sheik-Bahae, A. A. Said, D. J. Hagan, and E. W. Van Stryland, "Z-scan measurements of the anisotropy of nonlinear refraction and absorption in crystals," *Opt. Lett.* **18**, 194 (1993).
  29. S. J. Bepko, "Anisotropy of two-photon absorption in GaAs and CdTe," *Phys. Rev. B* **12**, 669 (1975).
  30. M. D. Dvorak, W. A. Schroeder, D. Anderson, A. L. Smirl, and B. S. Wherrett, "Measurement of the anisotropy of two-photon absorption coefficients in zincblende semiconductors," *IEEE J. Quantum Electron.* **30**, 256 (1994).
  31. D. C. Hutchings and B. S. Wherrett, "Theory and anisotropy of two-photon absorption in zinc-blende semiconductors," *Phys. Rev. B* **49**, 2418 (1994).
  32. D. C. Hutchings and B. S. Wherrett, "Theory of the polarization dependence of two-photon absorption in zinc-blende semiconductors," *J. Mod. Opt.* **41**, 1141 (1994).
  33. W. A. Schroeder, D. McCallum, D. Harken, M. Dvorak, D. Anderson, and A. Smirl, "Intrinsic and induced anisotropy of nonlinear absorption and nonlinear refraction in zinc blende semiconductors," *J. Opt. Soc. Am. B* **12**, 401 (1995).
  34. D. A. B. Miller, C. T. Seaton, M. E. Prise, and S. D. Smith, "Band-gap-resonant nonlinear refraction in III-V semiconductors," *Phys. Rev. Lett.* **47**, 197 (1981).
  35. M. Sheik-Bahae, J. Wang, and E. W. Van Stryland, "Nondegenerate optical Kerr effect in semiconductors," *IEEE J. Quantum Electron.* **QE-30**, 249 (1994).
  36. A. G. Aronov, D. E. Pikus, and D. Sh. Shekhter, "Quantum theory of free-electron dielectric constant in semiconductors," *Sov. Phys. Solid State* **10**, 645 (1968).
  37. D. H. Austin, S. McAfee, C. V. Shank, E. P. Ippen, and O. Teschke, "Picosecond spectroscopy of semiconductors," *Solid-State Electron.* **21**, 147 (1978).
  38. P. Amirtharaj and D. Seiler, "Optical properties of Semiconductors," in *Handbook of Optics* Vol. II, M. Bass, E. Van Stryland, D. Williams, and W. Wolf, eds. (McGraw-Hill, New York, 1995), Chap. 36, pp. 36.1-36.96.